JOC The Journal of Organic Chemistry

ARTICLE

pubs.acs.org/joc

Improper Hydrogen Bonded Cyclohexane C−H_{ax}···Y_{ax} Contacts: Theoretical Predictions and Experimental Evidence from ^{1}H NMR Spectroscopy of Suitable Axial Cyclohexane Models

Antonios Kolocouris,*[,†] Nikolaos Zervos,[†] Frank De Proft,[‡] and Andreas Koch[§]

[†]Faculty of Pharmacy, Department of Pharmaceutical Chemistry, University of Athens, Panepistimioupolis-Zografou, 15771 Athens, Greece

[‡]Eenheid Algemene Chemie, Faculteit Wetenschappen, Vrije Universiteit Brussel, Pleinlaan 2, B-1050 Brussels, Belgium

[§]Institut für Chemie, Universität Potsdam, Karl-Liebknecht-Strasse 24-25, D-14476 Potsdam (Golm), Germany

Supporting Information

ABSTRACT: C−H_{ax}···Y_{ax} contacts are a textbook prototype of steric hindrance in organic chemistry. The nature of these contacts is investigated in this work. MP2/6-31+G(d,p) calculations predicted the presence of improper hydrogen bonded C−H_{ax}···Y_{ax} contacts of different strength in substituted cyclohexane rings. To support the theoretical predictions with experimental evidence, several synthetic 2-substituted adamantane analogues (**1**−**24**) with suitable improper H-bonded C−H_{ax}···Y_{ax} contacts of different strength were used as models of a substituted cyclohexane ring. The ^{1}H NMR signal separation, $\Delta\delta(\gamma\text{-}CH_2)$, within the cyclohexane ring γ-CH_2s is raised when the MP2/6-31+G(d,p) calculated parameters, reflecting the strength of the H-bonded C−H_{ax}···Y_{ax} contact, are increased. In molecules with enhanced improper H-bonded contacts C−H_{ax}···Y_{ax}, like those having sterically crowded contacts (Y_{ax} = *t*-Bu) or contacts including considerable electrostatic attractions (Y_{ax} = O−C or O═C) the calculated DFT steric energies of the γ-axial hydrogens are considerably reduced reflecting their electron cloud compression. The results suggest that the proton H_{ax} electron cloud compression, caused by the C−H_{ax}···Y_{ax} contacts, and the resulting increase in $\Delta\delta(\gamma\text{-}CH_2)$ value can be effected not just from van der Waals spheres compression, but more generally from electrostatic attraction forces and van der Waals repulsion, both of which are improper H-bonding components.

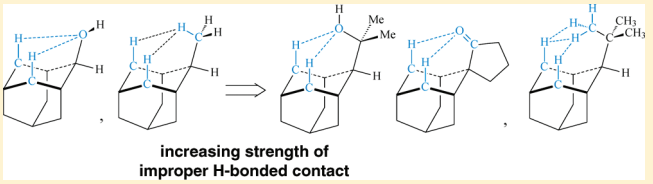

INTRODUCTION

Fundamental structural problems in organic chemistry, like the understanding of the forces leading to the relative stabilization of the different conformers in ethane and butane, are currently under intense research.[1] C(sp^3)−H···Y contacts are formed when the axial proton of a cyclohexane or any cyclohexane derivative in the chair conformation is replaced by substituent Y. The C−H_{ax}···Y_{ax} contacts are a textbook prototype of steric hindrance in organic chemistry. Calculations from Baerends group in ethane conformers showed that steric crowding is consistent with stronger Pauli repulsions.[1a] In a recent work,[2] the contacts between axial substituents Y and axial C−H bonds in cyclohexane derivatives, which are generally termed as only steric (van der Waals spheres crowding), were revisited. It was striking that the calculations located the overlap interactions $n(Y_{ax}) \rightarrow \sigma^*(C{-}H_{ax})$, that is, it was reported for the first time that the C−H_{ax}···Y_{ax} contacts are improper hydrogen bonded contacts[3−6] even in the most common axial cyclohexane derivatives (methyl cyclohexane, cyclohexanol, etc).[2,7] Improper or weak H-bonded X−H···Y contacts, which include often C−H donating groups, can cause mostly a shortening of the X−H bond in contrast to the elongation observed for strong polar hydrogen bonding (X, Y = N, O, F).[3−5]

A significant part of that paper[2] encompassed structures with contacts in which the improper hydrogen bonding character was enhanced because of a linker group. It was predicted that the orbital interaction $n(Y_{ax}) \rightarrow \sigma^*(C{-}H_{ax})$ and the strength of the hydrogen bonding contact would be increased by the addition of an appropriate bridging fragment X between the axial substituent Y_{ax} and the cyclohexane carbon C-1 and by constraining the conformation in such a way that the X_{ax}−Y bond vector bisects the cyclohexane ring and the lone pair orbital(s) (or electron cloud in general) of substituent Y can transfer electron charge to the $\sigma^*(C{-}H_{ax})$ antibonding orbitals (see the right-hand part structure depicted in Scheme 1).[2]

It was therefore intriguing for us to find experimental evidence for H-bonded contacts based on the different strength of H-bonding interactions that the calculations predicted for the different cyclohexane derivatives.

When an axial substituent is attached to the cyclohexane ring, a major effect of the C−H_{ax}···Y_{ax} contact in the ^{1}H NMR spectrum is to increase the difference between the chemical shifts of the axial and equatorial protons within the γ-methylene

Received: January 17, 2011
Published: April 12, 2011

Scheme 1. General Structure of Cyclohexane Derivatives with C−H_{ax}···Y−X_{ax} Contacts (Right-Hand Structure) Favoring Enhanced Improper H-Bonded Interactions (Blue Dotted Lines) Compared to the C−H_{ax}···Y_{ax} Contacts (Left-Hand Structure)

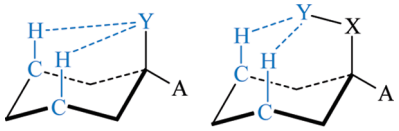

cy-Y_{ax} **cy-X_{ax}-Y**

Scheme 2. Synthetic Adamantane Derivatives 1−24 that Provide Models to Study Cyclohexane Improper H-Bonded C−H_{ax}···Y_{ax} Contacts using ^{1}H NMR Spectroscopy and Theoretical Models

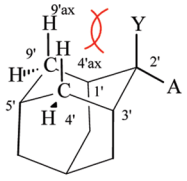

1: Y=**H** - A=H
2: Y=**C**H_3 - A=H
3: Y= C(**C**H_3)$_3$ - A=H
4: Y=**C**N -A=H
5: Y=**C**N -A=Me
6: Y=**O**H - A=H
7: Y=**O**Me - A=H
8: Y=**O**H - A=Me
9: Y=**O**H - A=*t*-Bu
10: Y=**O**COMe - A=H
11: Y=**N**H_2 - A=H
12: Y=**N**Me_2 - A=H
13: Y=**N**HCOMe - A=H
14: Y=**F** - A=H
15: Y=**Cl** - A=H
16: Y=**S**H - A=H
17: Y=**S**Me - A=H
18: Y=CMe_2**O**H - A=H
19: Y=C**O**Me - A=H
20: Y,A=C**O**$(CH_2)_2$
21: Y,A=C**O**$(CH_2)_3$
22: Y,A=C**O**$(CH_2)_4$
23: Y,A=C**O**$CH_2C_6H_4$
24: Y,A=C**O**$(CH_2)_2C_6H_5$

unit. In the present work, we examine whether the changes in the proton signal separation within the cyclohexane ring γ-CH_2 group are resulted from improper H-bonded C−H_{ax}···Y_{ax} contacts of different strength.[8] To observe this effect, the ^{1}H NMR spectrum of the axial conformer of the desired cyclohexane derivative, being accessible only at low temperatures when ring inversion is a slow process,[9] requires analysis if the existing population of the axial conformer and spectral resolution permits.

However, 2-adamantane derivatives represent models of axially substituted cyclohexanes;[10] in these molecules, substituent Y is axial in the adamantane cyclohexane ring 1′-2′-3′-4′-5′-9′ (Scheme 2). This observation motivated us to synthesize and analyze calculated parameters and the ^{1}H NMR spectra of several 2-adamantane analogues as models of the relevant parent cyclohexane derivatives, which represent a subset of the structures included in Scheme 1. In the present work our aim was (a) to check, using the appropriate model systems, if changes related to the proton C−H_{ax} chemical shift follow changes in the MP2/6-31+G(d,p) calculated parameters, reflecting the strength of the improper H-bonded contact C−H_{ax}···Y_{ax} interaction[8] and (b) to investigate the nature of the fundamental for organic chemistry C−H_{ax}···Y_{ax} contacts using the results of MP2 theory and a recent DFT steric analysis model, which will be described below.

RESULTS AND DISCUSSION

In this work, the 2-adamantane analogues **1**−**24** (Scheme 2) were prepared as models of the relevant parent cyclohexane C−H_{ax}···Y_{ax} contacts.[2] The ^{1}H NMR spectra of the adamantane derivatives **1**−**24** enabled a study on how the proton chemical shifts of the γ-methylene were affected by the various C−H_{ax}···Y contacts; the proton signal separation within the cyclohexane ring γ-CH_2 group, $\Delta\delta(\gamma\text{-}CH_2)$, is the experimental quantity that was obtained simply enough by measuring the proton resonance separation within the 4′,9′-CH_2[11] in the ^{1}H NMR spectra of compounds **1**−**24** recorded easily at 298 K.[12]

The study of intramolecular hydrogen bonding contacts using NMR spectroscopy has inherent difficulties related to the definition of the reference system. In addition to the simplicity in obtaining the spectra at 298 K and in the data interpretation, the models used in this work provide an additional benefit. In the unsubstituted cyclohexane chair, the axial proton is located upfield with respect to the geminal equatorial proton, so the chemical shift difference between axial and equatorial protons is negative. A C−H_{ax}···Y_{ax} contact will mostly shift the axial proton resonance in a downfield direction making $\Delta\delta(\gamma\text{-}CH_2)$ smaller and more positive. In each cyclohexane ring subunit of the parent adamantane, the protons of a CH_2 group are chemically equivalent, that is, the $\Delta\delta(\gamma\text{-}CH_2)$ value is zero in the parent "unperturbed" adamantane molecule (Scheme 2, Y = A = H). A C−H_{ax}···Y_{ax} contact will result in a positive value of $\Delta\delta(\gamma\text{-}CH_2)$ that will certainly be higher in magnitude than that of the relevant cyclohexane molecules. The situation is similarly convenient for the evaluation of the changes in hybridization, bond length, charges, and DFT steric energies (see below for the description).

As was mentioned above, the contacts between the axial substituents Y and the axial C−H bonds in cyclohexane derivatives were traditionally considered to include only van der Waals spheres crowding (which is usually attributed to Pauli repulsions[1a]) and similarly the observed boost in chemical shift differences, $\Delta\delta(\gamma\text{-}CH_2)$, was attributed to steric compression. This picture will be re-examined through the evidence provided in this work.[12]

It has been proposed that the identification of a delocalization interaction $n(Y) \rightarrow \sigma^*(C-H)$ or $\sigma(C-H) \rightarrow \sigma^*(C-H)$ assures the presence of an improper hydrogen bonded contact.[7] In an improper H-bonded contact, the calculated parameters that reflect its strength are the increase in % s-character, the contraction of the C−H_{ax} bonds, and the energy values of hyperconjugative interactions; an increase in proton positive charge is also consistent with a boost in strength of a H-bonded contact.

The suggestion that the variance of the strength of the improper H-bonding contact follows the observed $\Delta\delta(\gamma\text{-}CH_2)$ values will be investigated by calculating (a) the increase in % s-character and the contraction of the C−H_{ax} bonds relative to the equatorial bonds in the cyclohexane-subunit of the adamantane ring and the magnitude of the hyperconjugative $n(Y_{ax}) \rightarrow \sigma^*(C-H_{ax})$ interaction(s), which locate theoretically an improper H-bonded contact, using natural bond orbital analysis[7a] and (b) the steric energies of the interacting atoms inside the contact C−H_{ax}···Y_{ax} using Liu's recent DFT steric analysis model[13] according to which the total energy comes from the independent

dx.doi.org/10.1021/jo102353f |*J. Org. Chem.* 2011, 76, 4432–4443

contribution of three effects—steric, quantum, and electrostatic. Using this DFT steric analysis approach, the steric effect is precisely defined by the Weizsäcker kinetic energy[14] as will be described below and also in the Methods section. Liu's partition scheme was applied in molecules **1**−**24** to calculate the DFT steric energies of the γ-hydrogens included by the C−H_{ax}···Y_{ax} contacts.

NBO and Proton Chemical Shifts Analysis. The proton signal separation values within the cyclohexane ring γ-CH_2 group, that is, the proton resonance separation values within the 4′,9′-CH_2, $\Delta\delta(\gamma\text{-}CH_2)$, recorded easily at 298 K for molecules **1**−**24** are included in Table 1.

The geometries of the conformational ground states of molecules **1**−**24** were optimized using the MP2 theory to include electron correlation effects and the 6-31+G(d,p) basis set.[15] The natural bond orbital (NBO) analysis,[7a] which analyzes the molecular wave function to a set of localized bond and lone pair orbitals, was applied at the geometry-optimized structures of the global minima at the same level of theory (MP2/6-31+G**). The NBO analysis revealed that in all of the molecules the C−H_{ax}···Y contacts cause an increase in % s-character and a contraction of the C−H_{ax} bonds relative to the equatorial bonds and an increase in proton positive charge of axial relative to equatorial hydrogens in the cyclohexane-subunit of the adamantane ring [the corresponding values of Δ% s-char. = (% s-char. $C_{4'}$−H_{ax} − % s-char. $C_{4'}$−H_{eq}), $\Delta r_{4'} = r(C_{4'}\text{−}H_{ax}) - r(C_{4'}\text{−}H_{eq})$, $\Delta r_{9'} = r(C_{9'}\text{−}H_{ax}) - r(C_{9'}\text{−}H_{eq})$ and $\Delta q = q(H_{4'ax}) - q(H_{4'eq})$ or $q(H_{9'ax}) - q(H_{9'eq})$ are included in Table 1].[16] In compounds **1**−**24**, the C−H_{ax}···Y contact distances were smaller than the sum of the van der Waals radii[17] of the relevant atoms which is always encountered in H-bonded contacts. The existence of hyperconjugative interactions $n(Y) \rightarrow \sigma^*(C\text{−}H_{ax})$ in molecules **1**−**24** was examined by the NBO method at the MP2/6-31+G** level of theory (and also at the B3LYP/6-31+G**, see ref 16 and the Supporting Information). The calculations located overlap interactions in all compounds **1**−**24**, suggesting the presence of improper hydrogen bonding in C−H_{ax}···Y contacts (see Table 1 and Tables S1−S3 in the Supporting Information). Although the first effects, that is, the inequality $r_{H\cdots Y} < r_{vdw,H} + r_{vdw,Y}$, the increase in the % s-character, and the contraction of the C−H bond, are common in improper H-bonded contacts,[18] the identification of a covalent component in a C−H···Y contact, that is, the calculation of a hyperconjugative interaction $n(Y) \rightarrow \sigma^*(C\text{−}H)$, is diagnostic for the presence of improper hydrogen bonding.[7] However, the degree of hyperconjugative electron transfer is only one of the effects contributing to improper hydrogen bonding, the strength of which is also reflected by the increase in the % s-character and the contraction of the C−H_{ax} bond length.

In compounds **2** and **3**, the calculations predicted a dihydrogen bonding[19] interaction in the C−H_{ax}···H−C_{alkyl} contacts; electron density from the orbital σ(C−H) of the Lewis base C−H delocalizes into the antibonding orbital σ^*(C−H) of the Lewis acid C−H. The presence of attractive C−H···H−C interactions in the alkane dimers was theoretically predicted some years ago,[20] and it has been recently proposed that the identification of a delocalization interaction $\sigma(C\text{−}H) \rightarrow \sigma^*(C\text{−}H)$ assures the presence of a dihydrogen bonded contact.[21] The strength of the dihydrogen-bonded interaction of the C−H_{ax}···H−C contact increases on going from the primary methyl to the tertiary *t*-Bu group. This is reflected from the shorter C−H···H−C distances and the higher increase in the % s-character, the contraction of the C−H_{ax} bonds relative to the equatorial bonds of the cyclohexane-subunit of adamantane ring and the higher values of second order perturbative energies (Table 1). Comparison of the second order perturbative interactions revealed that the stronger orbital interaction $\sigma(C\text{−}H)_{alkyl} \rightarrow \sigma^*(C\text{−}H_{ax})$ (E = 0.59 kcal mol^{-1} in **3** compared to 0.24 kcal mol^{-1} in **2**) resulted from the more effective orbital overlapping; while the energy difference between the interacting orbitals is similar in all cases ($\varepsilon_{\sigma^*(C\text{-}Hax)} - \varepsilon_{\sigma(C\text{-}Hax)}$ = 1.40−1.41), the matrix elements $\langle\sigma|F|\sigma^*\rangle$ are larger on going from **2** (Y = Me) to **3** (Y = *t*-Bu) (0.016 au in **2** vs 0.026 au in **3**, see Table S1 in the Supporting Information). The stronger dihydrogen bonding interaction C−H_{ax}···H−C in **3** compared to that of **2** causes a larger proton chemical shift separation within the cyclohexane ring γ-CH_2 group; the signal separation $\Delta\delta(\gamma\text{-}CH_2)$ was 0.50, and 0.45 ppm in compounds **3** and **2** respectively (Table 1).

When the acceptor group is Y = OR, NR_2 and the second row lone-pair bearing heteroatom is directly connected to the cyclohexane ring-subunit, the weak interaction [$n(Y_{ax}) \rightarrow \sigma^*(C\text{−}H_{ax})$, $E \leq 0.63$ kcal mol^{-1}] is located,[22] which nevertheless indicates the presence of a hydrogen bonded C−H_{ax}···Y_{ax} contact. The hyperconjugative interaction efficiency was increased on going from Y = F and OH or OMe to NH_2 or NMe_2, which is consistent with the basicity order of these groups. The % s-character and the contraction of the C−H_{ax} bonds relative to the equatorial bonds follow the same order. While the calculated effect of lone pair bearing heteroatom raises from oxygen and fluorine to nitrogen, the value of the proton signal separation within the cyclohexane ring γ-CH_2 group $\Delta\delta(\gamma\text{-}CH_2)$ is 0.45 ppm in **11** (Y = NH_2) and 0.53 and 0.54 ppm in **14** (Y = F) and **6** (Y = OH), respectively. It seems that this order of experimental values is not consistent with the greater improper hydrogen bonding efficacy of nitrogen in **11**. However, the experimental value reflects the averaging between three low energy conformers with the global minimum having the lone pair bisecting cyclohexane ring and the other two, being a little higher in energy, having a N−H bond instead orienting inside the cyclohexane ring. Indeed, the stronger effect of lone pair bearing nitrogen is manifested experimentally in **12** (Y = NMe_2) with $\Delta\delta(\gamma\text{-}CH_2)$ = 0.79 ppm, since this compound is conformationally homogeneous with nitrogen lone pair bisecting cyclohexane ring. In nitrile **4**, a CH/π improper hydrogen bonding interaction is present as suggested from calculated and experimental values.

An alkyl group at the geminal cyclohexane C-1 position pushes the axial group toward C−H_{ax} bond and reduces the contact distance C−H_{ax}···Y. This buttressing effect resulting in the enhancement of the hyperconjugative energy and the other characteristic improper hydrogen bonding interaction parameters (Δ% s char., Δr). The value of $\Delta\delta(\gamma\text{-}CH_2)$ increases consistently from 0.54 ppm in **6** (Y = OH, A = H) to 0.63 ppm in **8** (Y = OH, A = Me) and 0.79 ppm in **9** (Y = OH, A = *t*-Bu). Upon capping heteroatom lone pair, in the acetylated derivatives **10** (Y = OAc, A = H) and **13** (Y = NHAc, A = H), the strength of the contact is seriously reduced and the relevant values of $\Delta\delta(\gamma\text{-}CH_2)$ are 0.25 and 0.28 ppm, respectively.

When the interacting atom of the Y group in C−H_{ax}···Y contacts (Scheme 1, Table 1) changes from a second row to a third row lone-pair bearing heteroatom[23] (Y = SR, Cl in compounds **15**−**17**), a substantial elongation of contact distances by 0.2−0.5 Å and an increase in contact angles by 5−6° is

Table 1. Selected Structural Parameters[a−c] and Hyperconjugative Energies for the Cyclohexane Ring C−H_{ax}···Y Contacts Included in the Adamantane Derivatives 1−24 Calculated at the MP2/6-31G+ Level; in Addition ^{1}H Chemical Shifts ($CDCl_3$)[d] and Signal Separation of the γ-CH_2 Pairs[e] of Adamantane Cyclohexane Ring Subunits for Molecules 1−24**

system	C4−H_{ax}, C9−H_{ax} C4−H_{eq}, C9−H_{eq}	$r_{C4'Hax\cdots Y}$, $r_{C9'Hax\cdots Y}$ Å	$\theta_{C4'Hax\cdots Y}$, $\theta_{C9'Hax\cdots Y}$ deg	$\Delta r_{4'}$,$\Delta r_{9'}$[a] mÅ	Δ% s-char.[b]	Δq[c] *m*e	hyperconjugative interaction kcal mol^{-1}	$\delta_{4',9'ax}$, $\delta_{4',9'eq}$[e]	Δδ(γ-CH_2)[f]
1 (Y_1=H, A=H)	1.0955, 1.0955 1.0955, 1.0955	2.54, 2.54	89.0, 89.0	0	0	0	–	1.75, 1.75	0
2 (Y_1=CH_3, A=H)	1.0939, 1.0939 1.0957,1.0957	2.25, 2.25	113.2, 113.2	−1.8, −1.8	0.38, 0.38	0.3, 0.3	$E[\sigma(C-H)_{Me} \rightarrow \sigma^*(C4'-H_{ax})\ ] = 0.24$ $E[\sigma(C-H)_{Me} \rightarrow \sigma^*(C9'-H_{ax})\ ] = 0.24$	1.91, 1.46	0.45
3 (Y_1= $C(CH_3)_3$, A=H)	1.0893,1.0934 1.0964, 1.0964	2.33, 2.12	125.7, 131.6	−10.1	1.16, 0.60	5.5, −2.6	$E[\sigma(C4'-H_{ax}) \rightarrow \sigma^*(C2'-H)_{t\text{-}Bu}]^g = 0.10$ $E[\sigma(C4'-H_{ax}) \rightarrow \sigma^*(C2'-H)_{t\text{-}Bu}]^g = 0.34$ $E[\sigma(C9'-H_{ax}) \rightarrow \sigma^*(C2'-H)_{t\text{-}Bu}] = 0.58$ $E[\sigma(C2'-H)_{t\text{-}Bu} \rightarrow \sigma^*(C4'-H_{ax})]^g = 0.53$ $E[\sigma(C2'-H)_{t\text{-}Bu} \rightarrow \sigma^*(C4'-H_{ax})]^g = 0.20$ $E[\sigma(C2'-H)_{t\text{-}Bu} \rightarrow \sigma^*(C9'-H_{ax})] = 0.59$	2.03, 1.53	0.5
4 (Y_1= CN, A=H)	1.0943, 1.0943 1.0949, 1.0949	2.68, 2.68	96.1, 96.1	−0.6, −0.6	0.45, 0.45	10.8, 10.9	$E[\pi(C\equiv N) \rightarrow \sigma^*(C4'-H_{ax})] = 0.18$ $E[\pi(C\equiv N) \rightarrow \sigma^*(C9'-H_{ax})] = 0.18$	2.14, 1.73	0.41
5 (Y_1= CN, A=Me)	1.0937, 1.0937 1.0951, 1.0951	2.55, 2.55	96.9, 96.9	−1.4, −1.4	0.62, 0.62	13.9, 13.9	$E[\pi(C\equiv N) \rightarrow \sigma^*(C4'-H_{ax})] = 0.11$ $E[\pi(C\equiv N) \rightarrow \sigma^*(C9'-H_{ax})] = 0.11$	2.27, 1.78	0.49
6 (Y_1=OH, A=H)	1.0922, 1.0928 1.0955, 1.0955	2.55, 2.63	96.4, 96.0	−3.3, −2.7	0.76, 0.54	25.3, 18.1	$E[n_a(O) \rightarrow \sigma^*(C4'-H_{ax})] = 0.32$ $E[n_\beta(O) \rightarrow \sigma^*(C9'-H_{ax})] = 0.28$ $\alpha = sp^{1.15}, \beta = p$	2.07, 1.53	0.54
7 (Y_1=OMe, A=H)	1.0960, 1.0958 1.0953, 1.0951	2.53, 2.62	96.4, 96.4	0.7, 0.7	0.81, 0.52	24.6, 16.0	$E[n_a(O) \rightarrow \sigma^*(C4'-H_{ax})] = 0.42$ $E[n_\beta(O) \rightarrow \sigma^*(C9'-H_{ax})] = 0.22$ $\alpha = sp^{1.44}, \beta = p$	2.01, 1.47	0.54
8 (Y_1=OH, A=Me)	1.0912, 1.0916 1.0958, 1.0958	2.43, 2.51	97.1, 96.7	−4.6, −4.2	1.04, 0.83	30.3, 22.8	$E[n_a(O) \rightarrow \sigma^*(C4'-H_{ax})] = 0.50$ $E[n_\beta(O) \rightarrow \sigma^*(C9'-H_{ax})] = 0.35$ $\alpha = sp^{1.18}, \beta = p$	2.15, 1.52	0.63
9 (Y_1=OH, A=*t*-Bu)	1.0893, 1.0910 1.0963, 1.0961	2.31, 2.43	97.0, 96.2	−7.0, −5.1	1.39, 0.91	34.6, 17.4	$E[n_a(O) \rightarrow \sigma^*(C4'-H_{ax})] = 0.63$ $E[n_\beta(O) \rightarrow \sigma^*(C9'-H_{ax})] = 0.33$ $\alpha = sp^{1.22}, \beta = p$	2.26, 1.47	0.79
10 (Y_1= OAc, A=H)	1.0932, 1.0938 1.0954, 1.0953	2.55, 2.60	96.1, 96.1	−2.2, −1.5	0.54, 0.34	14.8, 7.5	$E[n_a(O) \rightarrow \sigma^*(C4'-H_{ax})] = 0.33$ $E[n_\beta(O) \rightarrow \sigma^*(C9'-H_{ax})] = 0.16$ $\alpha = sp^{0.70}, \beta = p$	1.87, 1.62	0.25
11 (Y_1= NH_2, A=H)	1.0919, 1.0919 1.0958, 1.0958	2.62, 2.62	96.7, 96.7	−3.9, −3.9	0.84, 0.84	25.7, 25.7	$E[n_a(N) \rightarrow \sigma^*(C4'-H_{ax})] = 0.50$ $E[n_\alpha(N) \rightarrow \sigma^*(C9'-H_{ax})] = 0.50$ $\alpha = sp^{4.28}$	1.97, 1.52	0.45
12 (Y_1= NMe_2, A=H)	1.0930, 1.0930 1.0961, 1.0961	2.62, 2.62	97.6, 97.6	−3.1, −3.1	0.79, 0.79	19.4, 19.4	$E[n_a(N) \rightarrow \sigma^*(C4'-H_{ax})] = 0.43$ $E[n_\alpha(N) \rightarrow \sigma^*(C9'-H_{ax})] = 0.43$ $\alpha = sp^{5.84}$	2.28, 1.41	0.87
13 (Y_1= NHAc, A=H)	1.0951, 1.0964	2.70, 2.74	95.9, 93.7	−0.1, 1.1	0.08, −0.15	−3.6, −20.8	$E[n_\alpha(N) \rightarrow \sigma^*(C4'-H_{ax})] = 0.31$	1.89, 1.61	0.28

dx.doi.org/10.1021/jo102353f J. Org. Chem. 2011, 76, 4432–4443

Table 1. Continued

system	C4−H_{ax}, C9−H_{ax} C4−H_{eq}, C9−H_{eq}	$r_{C4'Hax\cdots Y}$, $r_{C9'Hax\cdots Y}$ Å	$\theta_{C4'Hax\cdots Y}$, $\theta_{C9'Hax\cdots Y}$ deg	$\Delta r_{4'}$,$\Delta r_{9'}$ [a] mÅ	Δ% s-char. [b]	Δq [c] *m*e	hyperconjugative interaction kcal mol^{-1}	$\delta_{4',9'ax}$, $\delta_{4',9'eq}$ [e]	$\Delta\delta(\gamma\text{-}CH_2)$ [f]
	1.0952, 1.0953						α = p		
14 (Y_1=F, A=H)	1.0928, 1.0928 1.0951, 1.0951	2.57, 2.57	95.6, 95.6	−2.3, −2.3	0.52, 0.52	19.1, 19.1	$E[n_a(F) \rightarrow \sigma^*(C4'-H_{ax})] = 0.10$ $E[n_a(F) \rightarrow \sigma^*(C9'-H_{ax})] = 0.10$	2.08, 1.55	0.53
							α = p		
15 (Y_1=Cl, A=H)	1.0928, 1.0928 1.0950, 1.0950	2.84, 2.84	101.6, 101.6	−2.2, −2.2	0.61, 0.61	15.7, 15.7	$E[n_a(Cl) \rightarrow \sigma^*(C4'-H_{ax})] = 0.14$ $E[n_a(Cl) \rightarrow \sigma^*(C9'-H_{ax})] = 0.14$ $E[n_\beta(Cl) \rightarrow \sigma^*(C4'-H_{ax})] = 0.46$ $E[n_\beta(Cl) \rightarrow \sigma^*(C9'-H_{ax})] = 0.46$ $E[n_\gamma(Cl) \rightarrow \sigma^*(C4'-H_{ax})] = 0.20$ $E[n_\gamma(Cl) \rightarrow \sigma^*(C9'-H_{ax})] = 0.20$	2.25, 1.55	0.7
							$\alpha = sp^{0.22}, \beta = \gamma = p$		
16 (Y_1=SH, A=H)	1.0937, 1.0926 1.0954, 1.0953	2.83, 2.89	102.1, 102.3	−1.7, −2.7	0.53, 0.71	10.0, 18.5	$E[n_a(S) \rightarrow \sigma^*(C4'-H_{ax})] = 0.46$ $E[n_a(S) \rightarrow \sigma^*(C9'-H_{ax})] = 0.17$ $E[n_\beta(S) \rightarrow \sigma^*(C4'-H_{ax})] = 0.16$ $E[n_\beta(S) \rightarrow \sigma^*(C9'-H_{ax})] = 0.95$	2.19, 1.51	0.68
							$\alpha = sp^{0.51}, \beta = p$		
17 (Y_1=SMe, A=H)	1.0940,1.0930 1.0955,1.0956	2.83, 2.89	102.2, 102.4	−1.5, −2.6	0.50, 0.71	10.8, 18.2	$E[n_a(S) \rightarrow \sigma^*(C4'-H_{ax})] = 0.50$ $E[n_a(S) \rightarrow \sigma^*(C9'-H_{ax})] = 0.23$ $E[n_\beta(S) \rightarrow \sigma^*(C9'-H_{ax})] = 0.98$	2.18, 1.51	0.67
							$\alpha = sp^{0.51}, \beta = p$		
18 (Y_2=CMe_2OH, A=H)	1.0902, 1.0902 1.0966, 1.0966	2.35, 2.35	118.8, 118.8	−6.4, −6.4	1.54, 1.54	37.5, 37.4	$E[n_a(O) \rightarrow \sigma^*(C4'-H_{ax})] = 1.22$ $E[n_a(O) \rightarrow \sigma^*(C9'-H_{ax})] = 1.22$ $E[n_\beta(O) \rightarrow \sigma^*(C4'-H_{ax})] = 0.51$ $E[n_\beta(O) \rightarrow \sigma^*(C9'-H_{ax})] = 0.51$	2.18, 1.53	0.65
							$\alpha = sp^{1.16}, \beta = p$		
19 (Y_2=COMe, A=H)	1.0898,1.0950 1.0959,1.0956	2.38, 2.95	118.0, 112.9	−6.1, −0.6	1.55, 0.41	39.4, 7.9	$E[n_a(O) \rightarrow \sigma^*(C4'-H_{ax})] = 0.64$ $E[n_\beta(O) \rightarrow \sigma^*(C4'-H_{ax})] = 0.95$	1.75, 1.57	0.2
							$\alpha = sp^{0.75}, \beta = p$		
							$E[\pi(C{=}O \rightarrow \sigma^*(C4'-H_{ax})] = 0.11$ $E[\pi(C{=}O \rightarrow \sigma^*(C9'-H_{ax})] = 0.18$		
20 (Y_2,A =CO$(CH_2)_2$)	1.0930, 1.0930 1.0959, 1.0959	2.58, 2.58	121.6, 121.6	−2.9, −2.9	0.93, 0.93	27.5, 27.6	$E[n_a(O) \rightarrow \sigma^*(C4'-H_{ax})] = 0.19$ $E[n_a(O) \rightarrow \sigma^*(C9'-H_{ax})] = 0.19$ $E[n_\beta(O) \rightarrow \sigma^*(C4'-H_{ax})] = 0.44$ $E[n_\beta(O) \rightarrow \sigma^*(C9'-H_{ax})] = 0.45$	2.18, 1.62	0.56
							$\alpha = sp^{0.78}, \beta = p$		
							$E[\pi(C{=}O \rightarrow \sigma^*(C4'-H_{ax})] = 0.22$ $E[\pi(C{=}O \rightarrow \sigma^*(C9'-H_{ax})] = 0.21$		

dx.doi.org/10.1021/jo102353f |*J. Org. Chem.* 2011, 76, 4432–4443

Table 1. Continued

system	C4−H_{ax}, C9−H_{ax} C4−H_{eq}, C9−H_{eq}	$r_{C4'Hax\cdots Y}$, $r_{C9'Hax\cdots Y}$ Å	$\theta_{C4'Hax\cdots Y}$, $\theta_{C9'Hax\cdots Y}$ deg	$\Delta r_{4'}$,$\Delta r_{9'}$ [a] mÅ	Δ% s-char.[b]	Δq[c] *m*e	hyperconjugative interaction kcal mol^{-1}	$\delta_{4',9'ax}$, $\delta_{4',9'eq}$ [e]	$\Delta\delta(\gamma\text{-}CH_2)$[f]
21 (Y_2,A=C**O**$(CH_2)_3$)	1.0893,1.0922 1.0962,1.0959	2.32, 2.46	120.2, 119.3	−6.9, −3.7	1.74, 1.14	44.1, 27.2	$E[n_a(O)\rightarrow\sigma^*(C4'-H_{ax})] = 0.82$ $E[n_a(O)\rightarrow\sigma^*(C9'-H_{ax})] = 0.27$ $E[n_\beta(O)\rightarrow\sigma^*(C4'-H_{ax})] = 1.20$ $E[n_\beta(O)\rightarrow\sigma^*(C9'-H_{ax})] = 0.20$ $\alpha = sp^{0.74}$, β = p $E[\pi(C{=}O\rightarrow\sigma^*(C9'-H_{ax})] = 0.65$	2.42, 1.38	1.04
22 (Y_2,A=C**O**$(CH_2)_4$)	1.0898, 1.0965 1.0960, 1.0960	2.34, 3.17	117.1, 110.0	−6.2, 0.5	1.51, 0.10	33.0, −2.3	$E[n_a(O)\rightarrow\sigma^*(C4'-H_{ax})] = 0.53$ $E[n_\beta(O)\rightarrow\sigma^*(C4'-H_{ax})] = 0.50$ $\alpha = sp^{0.77}$, β = p $E[\pi(C{=}O\rightarrow\sigma^*(C4'-H_{ax})] = 0.54$	2.01, 1.57	0.44
23 (Y_2,A=C**O**$CH_2C_6H_4$)	1.0891,1.0923 1.0963,1.0959	2.30, 2.44	120.6, 119.7	−7.2, −3.6	1.83, 1.20	45.9, 27.8	$E[n_a(O)\rightarrow\sigma^*(C4'-H_{ax})] = 0.89$ $E[n_a(O)\rightarrow\sigma^*(C9'-H_{ax})] = 0.29$ $E[n_\beta(O)\rightarrow\sigma^*(C4'-H_{ax})] = 1.24$ $E[n_\beta(O)\rightarrow\sigma^*(C9'-H_{ax})] = 0.19$ $\alpha = sp^{0.74}$, β = p $E[\pi(C{=}O\rightarrow\sigma^*(C9'-H_{ax})] = 0.71$	2.80, 1.55	1.25
24 (Y_2,A=C**O**$(CH_2)_2C_6H_4$)	1.0888, 1.0960 1.0962, 1.0961	2.28, 2.98	118.9, 112.5	−7.4, −0.1	1.78, 0.30	40.7, 3.7	$E[n_a(O)\rightarrow\sigma^*(C4'-H_{ax})] = 0.84$ $\alpha = sp^{0.75}$, β = p $E[\pi(C{=}O\rightarrow\sigma^*(C4'-H_{ax})] = 0.33$ $E[\pi(C{=}O\rightarrow\sigma^*(C9'-H_{ax})] = 0.14$	2.21, 1.62	0.59

[a] $\Delta r_{4'} = r(C_{4'}-H_{ax}) - r(C_{4'}-H_{eq})]$. [b] Δ% s-char. = (% s-char. $C_{4'}-H_{ax}$ − % s-char. $C_{4'}-H_{eq}$)]. [c] $\Delta q = (qH_{ax} - qH_{eq})]$. [d] Spectra were recorded at 298 K and the signal of $CHCl_3$ residue was calibrated at 7.26 ppm. [e] Signals for 4′,9′-H of the compounds are in general broad doublets with $J_{gem} \approx 12$ Hz. [f] ^{1}H NMR chemical shift separation within γ-CH_2, $[\Delta\delta(\gamma\text{-}CH_2) = \Delta\delta_{4',9'} = \delta(H_{4',9'ax}) - \delta(H_{4',9'eq})$. [g] Correspond to different C−H bonds included by the same methyl or by different methyl groups inside a *t*-Bu group.

dx.doi.org/10.1021/jo102353f |*J. Org. Chem.* 2011, 76, 4432–4443

calculated (θ(C−H$_{ax}$···Y$_{ax}$ = 102−103°)). The interaction energy $E[n(Y_{ax}) \rightarrow \sigma^*(C-H_{ax})]$ increases by 0.2−0.7 kcal mol^{-1} because of the more effective orbitals overlapping ($F_{n\sigma^*}$).[24] Comparison of the NBO results for the relevant interactions $n(Y_{ax}) \rightarrow \sigma^*(C-H_{ax})$ revealed that the energy difference between the interacting orbitals is a little bit lower (i.e., by 1.1-fold), but more significantly the matrix elements $\langle n|F|\sigma^*\rangle$ have much higher values (1.7-fold) in the third row heteroatom bearing contacts (for example $\varepsilon_{\sigma^*(C\text{-}Hax)} - \varepsilon_{n(S)}$ = 1.22 au *vs* $\varepsilon_{\sigma^*(C\text{-}Hax)} - \varepsilon_{n(O)}$ = 1.09 au and $\langle n|F|\sigma^*\rangle$ = 0.017 au vs $\langle n|F|\sigma^*\rangle$ = 0.029 au in compounds **6** and **16**, respectively, see Table S1 in the Supporting Information).

Calculations on the complexes of hydrogen fluoride with H_2O, H_2S, $H_2C{=}O$ and $H_2C{=}S$ showed the preference of sulfur for a more "perpendicular" direction of approach to the donor atom.[25] In addition, a statistical analysis of C−H···X−R (X = halogen) and C−H···SR$_2$ contacts in crystal structures showed that their directionality disperses down to 120° compared to that of C−H···OR$_2$ contacts at 180°; in their highest incidence C−H···OR$_2$ contacts occur at 2.78 Å, C−H···SR$_2$ at 3.21 Å and C−H···Cl-R at 3.17 Å.[26] Recent comparative studies of the hydrogen bonded dimers Me$_2$O···HOMe, Me$_2$S···HOMe and S···HN showed that sulfur can be an almost equally good hydrogen bond acceptor as oxygen.[27] In agreement with these observations, the calculations predicted the stronger hyperconjugative interactions for the C−H···S contacts in compounds **16**, **17**, where the contact atom of the axial substituent is tetrahedral sulfur, compared to their oxygen analogs **6**, **7** (see also Tables S1, S3 in the Supporting Information). The examined experimental value of $\Delta\delta(\gamma\text{-}CH_2)$ increases consistently from 0.53 and 0.54, 0.54 ppm in **14** (Y = F) and **6**, **7** (Y = OH, OMe respectively) to 0.70 (Y = Cl) and 0.68, 0.67 ppm (Y = SH, SMe) in compounds **15** and **16**, **17**, respectively.

The adamantane derivatives **18**−**24**,[12] synthesized as models of the structure cy-X$_{ax}$−Y (see the right-hand part of Scheme 1) will be considered (Scheme 3).[28] The effect of the X$_{ax}$−Y bond when it bisects the cyclohexane ring and interacts more effectively with both the C−H$_{ax}$ bonds of cyclohexane ring will be examined comparatively to compounds **1**−**17**. Again, the strength of the improper H-bonded contacts and the relevant changes in experimental values of $\Delta\delta(\gamma\text{-}CH_2)$ will be analyzed.

The transition from compound **6** to compound **18** results in increased contact C−H$_{ax}$···O angles ($\theta_{C\text{-}Hax\cdots O}$ = 96° in **6** to $\theta_{C\text{-}Hax\cdots O}$ = 119° in **18**) and reduced contact distances (by ∼0.2−0.3 Å, Scheme 3) giving rise to more effective orbital overlapping (Scheme 4) and increased hyperconjugative energies by ∼1 kcal mol^{-1}, when the stronger orbital interactions $n(O) \rightarrow \sigma^*(C-H_{ax})$ for each compound are compared, because of the 2-fold higher matrix elements ($\langle n|F|\sigma^*\rangle$ = 0.020 au in compound **6** vs 0.040 au in compound **16**, see Table S1, Supporting Information) (Schemes 3 and 4). Thus, the improper H-bonding interactions strengthen considerably since the CMe$_2$−OH group is conformationally homogeneous and the C−OH bond bisects cyclohexane ring, resulting also in a significant raise of the % s-character, the contraction of the C−H$_{ax}$ bonds relative to the equatorial bonds and the axial proton positive charge changes (the values of the Δ% s-char. and Δq and of the C−H$_{ax}$ bond contraction changes from ∼0.7 and 18 *me* and ∼−3 Å in **6** to ∼1.5, 38 *me* and −6 Å in **18**) (Table 1, Scheme 3). The signal separation $\Delta\delta(\gamma\text{-}CH_2)$ was 0.54 in **6** whereas in compound **18** was 0.65 ppm (Table 1).

In the acetyl derivative **19** and the cyclohexanone derivatives **22**, **24**, the C=O bond eclipses the cyclohexyl C2′-C3′ bond

Scheme 3. Improper Hydrogen Bonded C−H$_{ax}$···O Contacts (Colored in Blue) in Some Axial Cyclohexane Models Including Gradual Structural Changes That Are Useful for Comparisons of the H-Bonding Strength

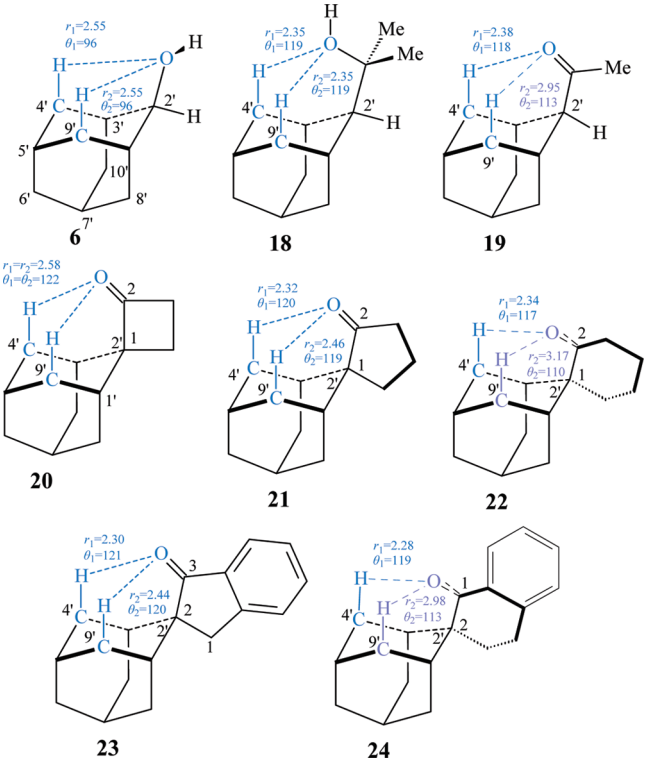

Scheme 4. Graphical Display of the Most Important Orbital Interactions $n(O) \rightarrow \sigma^*(C-H_{ax})$ for the Transition from 6 to 18; the Most Important Hyperconjugative Donations in 18 Are Clearly Depicted

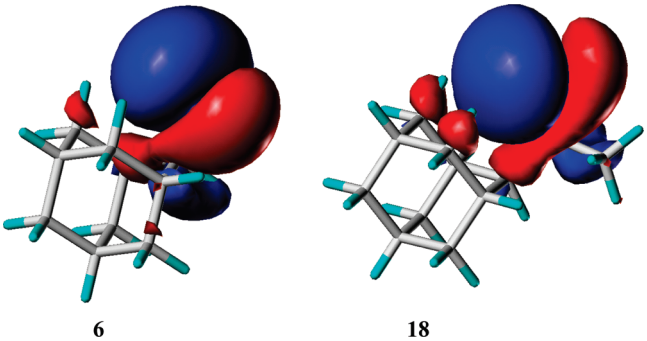

favoring improper H-bonding interactions with only one C−H$_{ax}$ bond compared to the compounds **21** and **23** in which the C=O bond bisects cyclohexane ring allowing the oxygen lone pair electrons and the π-bond of the carbonyl group to transfer electron charge to both C−H$_{ax}$ antibonding orbitals, according to the calculated hyperconjugative energies (Scheme 3, see Table 1 and Table S1 of the Supporting Information). In the cyclobutanone derivative **20**, the C=O bond vector also bisects the cyclohexane ring, but the contact distances are 0.1 − 0.3 Å longer resulting in weaker improper

dx.doi.org/10.1021/jo102353f |*J. Org. Chem.* 2011, 76, 4432–4443

Table 2. Steric Energies of the γ-Axial Hydrogens Included in the Various Improper H-Bonded C−H_{ax}···Y_{ax} Contacts of the Adamantane Derivatives 1−24

	$E_S[\rho(\vec{r})]$			
molecule	H_{4ax}	H_{9ax}	H_{4eq}	H_{9eq}
1 (Y = H, A = H)	0.485	0.485	0.485	0.485
2(Y = Me, A = H)	0.478	0.478	0.483	0.483
3 (Y = *t*-Bu, A = H)	0.472	0.468	0.483	0.482
4 (Y = CN, A = H)	0.476	0 0.476	0.483	0.484
5 (Y = CN, A = Me)	0.472	0.472	0.483	0.483
6 (Y = OH, A = H)	0.478	0.479	0.485	0.484
7 (Y = OMe, A = H)	0.478	0.478	0.484	0.484
8 (Y = OH, A = Me)	0.476	0.476	0.484	0.484
9 (Y = OH, A = *t*-Bu)	0.475	0.473	0.482	0.482
10 (Y = OCOMe, A =H)	0.478	0.478	0.484	0.484
11 (Y = NH_2, A = H)	0.476	0.476	0.484	0.484
12 (Y = NMe_2, A = H)	0.473	0.473	0.483	0.483
13 (Y = NHAc, A = H)	0.477	0.477	0.483	0.484
14 (Y = F, A = H)	0.482	0.481	0.484	0.484
15 (Y = Cl, A = H)	0.471	0.471	0.483	0.484
16 (Y = SH, A = H)	0.470	0.471	0.484	0.483
17 (Y = SMe, A = H)	0.469	0.471	0.484	0.484
18 (Y = CMe_2OH, A = H)	0.463	0.467	0.481	0.480
19 (Y = COMe, A = H)	0.475	0.466	0.483	0.483
20 (Y,A = $CO(CH_2)_2$)	0.472	0.472	0.483	0.483
21 (Y,A = $CO(CH_2)_3$)	0.468	0.464	0.482	0.482
22 (Y,A = $CO(CH_2)_4$)	0.465	0.473	0.481	0.483
23 (Y,A = $COCH_2C_6H_4$)	0.465	0.463	0.482	0.482
24 (Y,A = $CO(CH_2)_2C_6H_4$)	0.462	0.473	0.481	0.482

H-bonded C−H_{ax}···O contacts with respect to the cyclopentanone derivative **21** (Table 1). It is interesting to analyze comparatively the magnitude of some second order perturbative interactions. For example, the stronger orbital interaction $n(O) \rightarrow \sigma^*(C-H_{ax})$ in spirocyclopentanone derivative **21** (E = 1.20 kcal mol^{-1}) compared to 0.45 and 0.53 kcal mol^{-1} in spirocyclobutanone derivative **20** and spirocyclohexanone derivative **22**, respectively, resulted from the more effective orbital overlapping; while the energy difference between the interacting orbitals is similar in all cases ($\varepsilon_{\sigma^*(C\text{-}Hax)} - \varepsilon_{n(O)}$ = 1.18−1.21 au), the matrix elements $<n|F|\sigma^*>$ are larger on going from **20** or **22** to **21** (0.021 au in **20** and 0.022 au in **22** vs 0.035 au in **21**, see Table S1 in the Supporting Information). In cyclopentanone derivatives **21** and **23**, the % s-character, the axial proton positive charge, and the contraction of the C−H_{ax} bonds relative to the equatorial bonds (Table 1) are also considerably stronger than those in compounds **19**, **20**, **22**, and **24**. The stronger H-bonded contacts cause a more pronounced redistribution of electronic shielding within the cyclohexane ring γ-CH_2s effecting higher values of proton chemical shift separation within the cyclohexane ring γ-CH_2 group. Indeed, in compounds **19**, **20**, **22**, and **24**, the signal separation $\Delta\delta(\gamma\text{-}CH_2)$ was 0.20, 0.56, 0.44, and 0.59 ppm whereas in compounds **21** and **23** it was 1.04 or 1.25 ppm respectively (Table 1).[8] It is also striking to note the related calculated (Δ% s-char. and bond contraction values) and experimental values ($\Delta\delta(\gamma\text{-}CH_2)$) reflecting the stronger H-bonded contacts due to the C═O bonds in **21** and **23** compared to the C−O bond in **19**; in the former case, a more efficient interaction is allowed, because in addition to the oxygen lone pair(s) the π-bond of the carbonyl group electrons can also interact with C−H_{ax} bonds.

According to Table 1, the contact distances for compounds **2** and **4**−**17** range from 2.25 to 2.89 Å and the angles vary from 95.6 to 113.2°. For compounds **3** and **18**−**24**, the contact distances vary from 2.12 to 3.17 Å and the angles from 117.1 to 131.6°, due to the presence of X_{ax} bridge, which allow a more significant improper H-bonded interaction inside the C−H_{ax}···Y_{ax} contact (see Schemes 1, 3).

DFT Steric Analysis. The steric effect is one of the most widely used qualitative concepts in chemistry. According to Liu's DFT steric analysis,[13,14] the steric effect is quantitatively defined by the Weizsäcker kinetic energy which can be expressed as

$$E_S[\rho(\mathbf{r})] \equiv T_W[\rho(\mathbf{r})] = \frac{1}{8}\int \frac{|\nabla[\rho(\mathbf{r})]|^2}{\rho(\mathbf{r})} \qquad (1)$$

where $\rho(\mathbf{r})$ is the electron density of the system, and $\nabla\rho(\mathbf{r})$ denotes the density gradient. This Weizsäcker kinetic energy term shows the amount of kinetic energy compression that is applied to electrons in a given nuclear configuration as measured by the change in the electron density gradient normalized to the total density (it can be viewed as the corresponding boson kinetic energy where no Pauli principle exists).[13,14] The application of this description of steric effect has already recently applied successfully to describe the shape of model systems, some internal barriers of small organic molecules, S_N2 reaction barriers and the thermodynamic stability of branched compared to linear alkanes.[29]

In order to investigate the C−H_{ax}···Y_{ax} contacts with additional theoretical models, calculations of the DFT steric energies of the γ-axial hydrogens, that is, the $4'_{ax}$, $9'_{ax}$-H that interact with Y_{ax} group, were performed based to eq 1. DFT steric energies were calculated at B3LYP/6-31+G(d,p) level according to eq 1; atomic contributions were computed after decomposition of molecular steric energies in single-atom components[30] (according to eq 4−7, see the computational chemistry details in Methods section for the description of the theoretical model). The resulting values of Table 2 are in agreement with the ranking of the improper H-bonding strength presented above and provide the background for useful comparisons between the nature of the substituent and the nature of the C−H_{ax}···Y_{ax} contacts, as will be discussed into the next paragraphs.

The DFT steric energy values of equatorial hydrogens $4'_{eq}$, $9'_{eq}$-H that are not directly interacting with Y_{ax} group are similar and equal to those of the unperturbed adamantane molecule **1** (Y = H). The DFT steric energies of $4'_{ax}$, $9'_{ax}$-H were reduced, due to their improper hydrogen bonding interactions with Y_{ax} substituent. In compound **2**, the C−H_{ax}···Me contact reduces the DFT steric energies by ∼0.007 au compared to the adamantane molecule **1**; with respect to the methyl group, the *t*-Bu substituent in compound **3** caused a ∼2-fold higher reduction in the DFT steric energies of the γ-axial hydrogens, that is, the steric energies were reduced by 0.013 au with respect to the adamantane molecule **1**. The CH/π improper hydrogen bonded contacts in nitrile **4** caused a little-bit lower reduction in DFT steric energies compared to those effected from the methyl group in compound **2**.

We recall that differences in DFT steric energy or the Weizsäcker kinetic energy correspond to differences in kinetic energy compression that is applied to electrons effected from the different substituent Y.

dx.doi.org/10.1021/jo102353f |*J. Org. Chem.* 2011, 76, 4432–4443

In compounds **6** (Y = OH), **11** (Y = NH_2), and **14** (Y = F), DFT steric energies were reduced by ~0.007−0.009 au with respect to the adamantane values; an additional reduction in DFT steric energies was calculated for the NMe_2 group in compound **12** compared to NH_2 group in compound **11**. The buttressing effect of methyl and *t*-Bu substituents pushing the contact atom closer to γ-axial hydrogens and resulting in lowering further the DFT steric energies of γ-axial hydrogens is observed, through comparison of the corresponding contacts in compounds **6** and **8**, **9** and in compounds **4** and **5**.

In compounds **15**−**17**, the DFT steric energies were smaller by ~0.015 au when compared to those in adamantane molecule **1**. Thus, when the interacting atom of the Y group in C−H_{ax}···Y contacts changes from a second row (Y = OR, NH_2, F in compounds **6**, **7**, **11**, **14**) to a third row lone-pair bearing heteroatom (Y = SR, Cl in compounds **15**−**17**), steric energies were reduced by ~0.006−0.011 au.

The same reduction but more pronounced is observed when compounds **6** (Y = OH) and **18** (Y = CMe_2OH) are compared, where the DFT steric energies of the γ-axial hydrogens are reduced by 0.011−0.015 au through the change OH → CMe_2OH; similarly when going from compounds **19**, **20**, **22**, **24** to **21**, **23**, the DFT steric energies of the γ-axial hydrogens that are involved in improper H-bonding contacts are reduced by 0.007−0.013 au. Thus, in compounds **18** and **21**, **23**, the DFT steric energies were smaller by ~0.020 au with respect to those in the adamantane molecule **1**.

In all the cases considered it seems that the DFT steric energies are reduced at the expense of the increase in improper hydrogen bonding interaction.

In improper hydrogen bonding contacts the major C−H bond shortening contributors, which are the der Waals spheres repulsive forces and the increased electrostatic attraction between the positive H and negative C, prevail the lengthening contributors of the C−H bond, that is, the attractive interactions between the positive H of the C−H dipole and the electron-rich acceptor group Y and the hyperconjugative electron donation $n(Y) \rightarrow \sigma^*(C-H)$.[4,5]

It is striking to compare compounds **3** and **18**, **21**, **23** bearing significant improper hydrogen bonding contacts, according to the results included in Table 1. In compound **3**, the bulky *t*-Bu, which effects the largest der Waals spheres crowding in γ-axial hydrogens, triggers a reduction in their DFT steric energies by ~0.015 au compared to the relevant values in the adamantane molecule **1**. In compounds **18**, **21**, and **23**, which bear the most important improper H-bonded contacts, DFT steric energies were reduced even more, that is, by ~0.020 au with respect to adamantane **1**. In compounds **18**, **21**, and **23**, the C−H_{ax}···O contacts, which are included in the six-membered ring $H_{4'ax}-C_{4'}-C_{3'}-C_{2'}-C_{ax}-O$ (or the correcponding ring which contains $9'_{ax}$-CH groups instead of the $4'_{ax}$-CH groups, see Scheme 5), should be more relaxed from der Waals spheres repulsion compared to the C−H_{ax}···$(CH_3)_2$−CMe contacts in compound **3** (Scheme 5).

The data suggest that the t-Bu group in the C−H_{ax}···*t*-Bu contact (compound **3**) effects a compression in proton H_{ax} electron cloud which can be attributed mainly to der Waals spheres repulsion, whereas in the C−H_{ax}···O contacts of compounds **18**, **21**, and **23** electrostatic attractive forces are also likely to effect the compression. Thus, in the latter compounds the compression of proton H_{ax} electron cloud can also be effected by electrostatic attraction (a) from the electron-rich acceptor group C−O or C═O and (b) from the negative C of C−H_{ax} bond. The significant electropositive character of H in the cases

Scheme 5. Depiction of the Geometrical Features for the Improper H-Bonded C−H_{ax}···Y_{ax} Contacts Included by the Cyclohexane Ring Subunits 1′-2′-3′-4′-5′-9′ in Compounds 3, 18, and 21

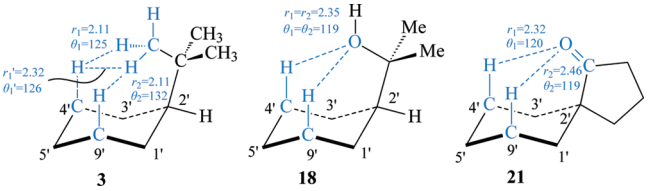

of compounds **18**, **21**, and **23**, that is, the electrostatic character of these C−H_{ax}···O contacts, is consistent with the highest calculated Δq charge values (Table 1).

It is striking that particularly in compounds **21** and **23**, $\Delta\delta(\gamma\text{-}CH_2)$ values are significantly higher, that is, 1.04 and 1.25 ppm respectively, compared to **3**. The traditional picture in the literature is that C−H_{ax}···Y_{ax} contacts and the downfield shifts of the γ-axial hydrogens are caused from van der Waals spheres repulsion. Although the origin of the shielding tensors that determine chemical shifts are under research in general,[31] the present data suggest that the increase in $\Delta\delta(\gamma\text{-}CH_2)$ value, caused by C−H_{ax}···Y_{ax} contacts, can be effected not just from der Waals spheres repulsion, but more generally from electrostatic attraction and der Waals spheres crowding forces, both of which are improper H-bonding components.

CONCLUSIONS

To summarize, in the present work, experimental evidence was presented associated with improper cyclohexane H-bonded contacts C−H_{ax}···Y_{ax} of different strength from using the NMR spectra of the prepared 2-substituted adamantane derivatives **1**−**24**, which represent the necessary cyclohexane models. The proton signal separation within the cyclohexane ring γ-CH_2s raises when the strength of the improper hydrogen bonding interactions in the C−H_{ax}···Y_{ax} contacts is increased.

Of considerable interest was the experimental and theoretical investigation of structures with contacts in which the improper hydrogen bonding character can be enhanced through a linker group, that is, the cyclohexane analogues Adam-X_{ax}−Y **3**, **18**−**24**. The strongest improper H-bonded contacts were observed in molecules **21** and **23**, where the X_{ax}−Y≡C═O bond vector bisects the cyclohexane ring subunit allowing the formation of a six-membered ring between the contact atoms O and γ-H_{ax}; significant signal separation, that is, 1.04 and 1.25 ppm, respectively, was measured, being consistent with the increased improper H-bonding character of these contacts.

It is striking that in compound **3**, with the bulky *t*-Bu effecting the largest van der Waals repulsion to γ-axial hydrogens, the reduction in DFT steric energies, which measures the electron cloud compression, was ~0.015 au compared to the relevant values in the adamantane molecule **1** and the $\Delta\delta(\gamma\text{-}CH_2)$ value was 0.50 ppm. In compounds **21** and **23**, which bear the most important improper H-bonded contacts, DFT steric energies were reduced even more, that is, by ~0.020 au with respect to adamantane molecule **1**, and the $\Delta\delta(\gamma\text{-}CH_2)$ values were 1.04 and 1.25 ppm, respectively. In the later molecules, C−H_{ax}···O contacts include less van der Waals spheres crowding. The electron cloud compression of the γ-axial hydrogens and the large chemical shift separations should be resulted from the electron cloud

withdraw of H_{ax} from the negative C of the C−H_{ax} bond and the acceptor group O−C or O═C; the enhanced electrostatic character of these contacts is consistent with the largest positive charges of γ-axial protons between the compounds in the series **1**−**24**. It is expected that in all molecules **1**−**24** bearing different substituents Y, a balance between van der Waals spheres repulsion and electrostatic attractive forces should work.

METHODS

Synthesis of Molecules 1−24. Compounds **6**, **7**, and **10**−**15** were synthesized according to conventional methods described several times in the literature.[32] Thus, compound **6** can be prepared through the $NaBH_4$ reduction of 2-adamantanone in ethanol; methylation of 2-adamantanol **6** with CH_3I/NaH in DMF afforded the methyl ether **7**; compound **11** was prepared through the Raney-Ni catalytic hydrogenation of 2-adamantanone oxime in ethanol; Borch-Hassid reductive amination of 2-adamantanamine **11** afforded the *N*,*N*-dimethyl derivative **12**; the treatment of 2-adamantanol **6** or 2-adamantanamine **11** with CH_3COCl/Et_3N in ether afforded the acetylated derivatives **10** or **13** respectively; the 2-fluoroadamantane **14** can be prepared through treatment of the alcohol **6** with DAST in CH_2Cl_2 at −78 °C; the treatment of 2-adamantanol with $SOCl_2$ afforded the 2-chloroadamantane **15**.

For the preparation of the 2-methyl-2-adamantanol **8** and the 2-*t*-Bu-2-adamantanol **9** the reaction of 2-adamantanone with methyl magnesium bromide or with t-BuLi respectively in ether can be used.[33]

For the synthesis of the ketone **19**, the 2-cyanoadamantane was used as a starting material (Scheme 6); 2-cyanoadamantane can be prepared through reaction of 2-adamantanone with tosyl methyl isocyanate in the presence of sodium ethoxide or potassium tert-butoxide; compound **5** was synthesized through methylation of the carbanion of 2-cyanoadamantane.[32c,34] Reaction of 2-cyanoadamantane with methyl lithium afforded the 2-acetyl adamantane **19**. Further reaction of **19** with methyl lithium afforded the tertiary alcohol **18** which represents a new compound (see Supporting Information for details of the preparation procedure and its ^1H and ^{13}C spectrum).

The preparation of compounds **8**, **9**[33] and **16**, **17**[35] and **20**−**22**[32c] and **23**, **24**[36] has been reported in the literature.

NMR Experiments. NMR experiments were conducted (i) on a 400 MHz machine operating at 400.13 MHz for obtaining the ^1H NMR spectra and (ii) on a 200 MHz machine operating at 50.32 MHz for the ^{13}C NMR spectra at 298 K. The ^1H NMR experiments were run at 298 K (400 MHz) by dissolving 5 mg of compound in 0.5 mL of $CDCl_3$. The ^{13}C NMR experiments were run at 298 K (50 MHz) by dissolving 20−30 mg of the compound in 0.5 mL of $CDCl_3$. ^1H chemical shifts (δ) are reported in ppm relative to the residual $CHCl_3$ signal at 7.26 ppm (s).

The 1D ^1H spectra (400 MHz) were acquired using a spectral width of 12 ppm, 2 s relaxation delay between cycles, 16 transients, 32K data points zero-filled to 64K data points before Fourier transformation (FT) and baseline correction. The 1D ^{13}C spectra (50 MHz) were recorded using 3 s relaxation delay, 512 transients, 64K data points, and 3 Hz line broadening prior to FT. DEPT-135 spectra (50 MHz) were obtained using 2 s relaxation delay, 800 transients, 32K data points, and 3 Hz line broadening prior to FT. The 2D experiments were run in $CDCl_3$ solutions (400 MHz) at a concentration of 0.02 M using a relaxation delay of 1.2 s. The assignments of ^1H and ^{13}C signals were achieved by the combined use of DEPT, 2D COSY and HMQC experiments. For the assignment of the ^1H NMR spectra, see also ref 11.

Computational Chemistry Details. All structures were fully optimized at the MP2/6-31+G** (and B3LYP/6-31+G**)[15] level using the GAUSSIAN 03 package (see Supporting Information). Frequency calculations were also performed at the B3LYP/6-31+G** to locate minima; no imaginary frequencies were located.

Scheme 6. Synthesis of Compound 18[a]

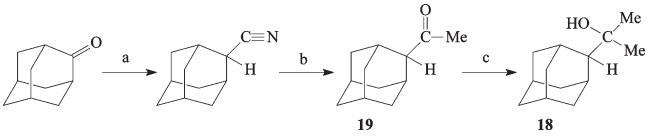

[a] Reagents and Conditions: (a) EtONa, TOSMIC, EtOH, THF, r.t., 2 h (quant.); (b) (i) MeLi, ether, Ar, 0 °C, then r.t. 90 min (ii) acetone, HCl 6N, reflux 2 h (78%); (c) (i) MeLi, ether, Ar, 0 °C, then r.t. 12 h (ii) NH_4Cl(aq), 0 °C (78%).

(a). NBO Analysis. The NBO 4.0 program[38] was used as implemented in the GAUSSIAN 03 package (see Supporting Information for the reference). NBO analysis was realized at the MP2/6-31+G** level. The NBO analysis transforms the canonical delocalized Hartree−Fock (HF) MOs into localized orbitals that "are closely tied to chemical bonding concepts". This process involves sequential transformation of nonorthogonal atomic orbitals (AOs) to the sets of "natural" atomic orbitals (NAOs), hybrid orbitals (NHOs) and bond orbital (NBOs). Each of these localized basis sets is complete and orthonormal. Importantly, these sets also describe the wave function in the most "economic" way since electron density and other properties are described by the minimal amount of filled orbitals in the most rapidly convergent fashion. Filled NBOs describe the hypothetical, strictly localized Lewis structure.

The interactions between filled and antibonding (or Rydberg) orbitals represent the deviation of the molecule from the Lewis structure and can be used as a measure of delocalizations. This method can give energies of hyperconjugative interactions from the standard second-order perturbation approach:

$$E(2) = -p_n\frac{\langle n|F|\sigma^*\rangle^2}{\varepsilon_{\sigma^*}-\varepsilon_n} \text{ or } -p_\sigma\frac{\langle \sigma|F|\sigma^*\rangle^2}{\varepsilon_{\sigma^*}-\varepsilon_\sigma} = -p_n\frac{F^2_{n\sigma}}{\Delta\varepsilon_{\sigma^*n}} \text{ or } -p_\sigma\frac{F^2_{\sigma\sigma}}{\Delta\varepsilon_{\sigma^*\sigma}} \quad (2)$$

where $F_{n\sigma^*}$ is the Fock matrix element between the n and σ^* NBO orbitals, ε_n and ε_{σ^*} are the energies of n and σ^* NBO's, and p_n is the population of the donor n orbital. A threshold of 0.10 kcal mol^{-1} for printing second order perturbation energies was used (the default value is 0.50 kcal mol^{-1}). Detailed descriptions of the NBO calculations are available.[36−39]

(b). Steric Effect Calculations. Liu recently proposed an energy partition scheme within the framework of density functional theory, assuming that the electronic energy comes from three independent effects—steric, electrostatic, and quantum (due to the exhange and correlation interaction)[13] according to eq 3:

$$E[\rho] = E_S[\rho] + E_e[\rho] + E_q[\rho] \quad (3)$$

where the steric contribution is found to be the Weizsäcker kinetic energy as described in the Introduction[14] (eq 1):

$$E_S[\rho(\mathbf{r})] \equiv T_W[\rho(\mathbf{r})] = \frac{1}{8}\int\frac{|\nabla[\rho(\mathbf{r})]|^2}{\rho(\mathbf{r})} \quad (1)$$

To obtain local values for this property for the purpose of probing the steric effect in certain region of a molecular system, integration can be performed over a particular region of the space to obtain its contribution to the global value.[30] By taking appropriate atomic domains defined in one or another way, one can define the atomic contributions to the steric energy, $E_{S,i}[\rho(\mathbf{r})]$:

$$E_{S,i}[\rho(\mathbf{r})] \equiv \frac{1}{8}\int_{\Omega_i}\frac{|\nabla[\rho(\mathbf{r})]|^2}{\rho(\mathbf{r})}\mathbf{dr} \quad (4)$$

dx.doi.org/10.1021/jo102353f |*J. Org. Chem.* 2011, 76, 4432–4443

in such a way so that:

$$E_S[\rho(\mathbf{r})] = \sum_{i=1}^{N} E_{S,i}[\rho(\mathbf{r})] \quad (5)$$

The fuzzy Voronoi polyhedra were used to define the atomic domains. It consists of the decomposition of the integral of eq 4 over the 3D space into a sum of integrations over single-atom components using a weight function $\omega_i(\mathbf{r})$ for nucleus i in the system at every point of space $\mathbf{r}$ in such a way that:

$$\sum_{i=1}^{N} \omega_i(\mathbf{r}) = 1 \quad (6)$$

In this scheme, the numerical integration of $E_S[\rho(\mathbf{r})]$ is determined as a sum of coordinates $E_{S,i}[\rho(\mathbf{r})]$:

$$E_S[\rho(\mathbf{r})] = \sum_{i=1}^{N} E_{S,i}[\rho(\mathbf{r})] \cong \frac{1}{8}\sum_{i=1}^{N}\int_{\Omega_i} \omega_i(\mathbf{r})\frac{|\nabla[\rho(\mathbf{r})]|^2}{\rho\mathbf{r}}\mathrm{d}\mathbf{r} \quad (7)$$

where $\omega_i(\mathbf{r})$ has the value 1 in the vicinity of its own nucleus, but vanishes in a continuous and well-behaved manner near any other nucleus. The atomic weights used here are derived from the fuzzy Voronoi polyhedra proposed by Becke, tuned by the Brag-Slater set of atomic radii and following Becke's suggestion to increase the radius of hydrogen to 0.35 Á. Such atomic definition has already been successfully applied for the calculation of overlap populations, bond orders, valences, or in several molecular energy decomposition schemes.

The steric energy and its atomic contributions were evaluated at the B3LYP/6-31+G(d,p)[15] level of theory using the optimized MP2/6-31+G(d,p) geometries, and the wave functions and densities obtained from the Gaussian 03 program. Each atom has been integrated using Chebyshev's integration for the radial part (40 points) and Levedev's quadrature (146 points) for the angular part. This level of methodology allows achieving accuracies of the order of 10^{-5} au. Additional information and references can be found in ref 30.

■ ASSOCIATED CONTENT

Supporting Information. Table S1 including the complete second order perturbation NBO analysis for the hyperconjugative interactions at the MP2/6-31+G** level and Tables S2, S3 include results of structure and NBO calculations at the B3LYP/6-31+G** level; Cartesian coordinates and electronic energies for the optimized conformational minima of compounds **1**−**24** at the MP2 and B3LYP levels; Representative ^{1}H NMR spectra. This material is available free of charge via the Internet at http://pubs.acs.org.

■ AUTHOR INFORMATION

Corresponding Author

*E-mail: ankol@pharm.uoa.gr.

■ ACKNOWLEDGMENT

This research activity was mainly supported through a research grant from Chiesi Hellas and secondarily by a research grant from the Special Account for Research Grants of the National and Kapodistrian University of Athens, Greece (research program code 70/4/5857 and 70/4/8775). F.D.P. acknowledges Dr. Shubin Liu and Dr. Miquel Torrent-Sucarrat for interesting discussions. He also gratefully acknowledges Dr. Torrent-Sucarrat for providing the program for the computation of the atomic and functional group steric contributions. F.D.P. acknowledges the Research Foundation Flanders (Belgium) FWO and the Vrije Universiteit Brussel (VUB) for continuous support to his research group.

■ REFERENCES

(1) See for example the work for ethane and *n*-butane. Some relevant references are: (a) Bickelhaupt, F. M.; Baerends, E. J. *Angew. Chem., Int. Ed.* **2003**, *42*, 4183. Mo, Y.; Gao, J. *Acc. Chem. Res.* **2007**, *40*, 113. Pophristic, V.; Goodman, L. *Nature* **2001**, *411*, 565. (b) Mo, Y. *J. Org. Chem.* **2010**, *75*, 2733.

(2) Kolocouris, A. *J. Org. Chem.* **2009**, *74*, 1842.

(3) (a) Desiraju, G. R.; Steiner, T. *The weak hydrogen bond in structural chemistry and biology*; IUCr Monographs on Crystallography, Vol. 9; Oxford University Press: Cambridge, 1999. (b) Steiner, T. *Angew. Chem., Int. Ed. Engl.* **1995**, *43*, 2311. (c) Panigrahi, S. K.; Desiraju, G. R. *PROTEINS: Struct. Funct. Bioinform.* **2007**, *67*, 128.

(4) Joseph, J.; Jemmis, E. D. *J. Am. Chem. Soc.* **2007**, *129*, 4620 and references cited therein.

(5) Between the different theories included in the citations of ref 4, a useful interpretation includes the combination of a hyperconjugative interaction $n(Y) \rightarrow \sigma^*(X-H)$ that weakens the X−H bond and a repolarization/rehybridization in which the X−H bond s-character increases, as H becomes more electropositive (Bent's rule), causing strengthening of the X−H bond. The second effect prevails, that is, improper H bonding is observed, when the hyperconjugation is relatively weak. See: (a) Alabugin, I. V.; Manorahan, M.; Peabody, S.; Weinhold, F. *J. Am. Chem. Soc.* **2003**, *125*, 5973. (b) Alabugin, I. V.; Manorahan, M. *J. Comput. Chem.* **2007**, *28*, 373.

(6) Experimental and theoretical studies identified the improper hydrogen bonded contacts C(sp^3)-H···Y (Y = O, N, S, π-donors), whilst simple systems such as $CH_4\cdots OH_2$, $CH_4\cdots NH_3$, $CH_4\cdots FH$, $CH_4\cdots SH_2$, $CH_4\cdots Cl^-$, $CH_4\cdots C_6H_6$ have been investigated. See for example: $CH_4\cdots OH_2$: (a) Novoa, J. J.; Planas, M.; Rovira, M. C. *Chem. Phys. Lett.* **1996**, *251*, 33. Masunov, A.; Dannenberg, J. J.; Contreras, R. H. *J. Phys. Chem. A* **2001**, *105*, 4737. $CH_4\cdots NH_3$: (b) Gu, Y.; Kar, T.; Scheiner, S. *J. Mol. Struct.* **2000**, *552*, 17. $CH_4\cdots FH$: (c) Vizioli, C.; Ruiz de Azua, M. C.; Giribet, C. G.; Contreras, R. H.; Turi, L.; Dannenberg, J. J.; Rae, I. D.; Weigold, J. A.; Malagoli, M.; Zanasi, R.; Lazzeretti, P. *J. Phys. Chem.* **1994**, *98*, 8558. $CH_4\cdots SH_2$: (d) Rovira, M. C.; Novoa, J. J. *Chem. Phys. Lett.* **1997**, *279*, 140. $CH_4\cdots Cl^-$: (e) Hiraoka, K.; Mizuno, R.; Iino, T.; Eguchi, D.; Yamade, S. J. *J. Phys. Chem. A* **2001**, *105*, 4887. C(sp^3)-H···π: (f) Utzat, K.; Bohn, R. K.; Michels, H. H. *J. Mol. Struct.* **2007**, *841*, 22. Tsuzuki, S.; Honda, K.; Uchimaru, T.; Mikami, M.; Fujii, A. *J. Phys. Chem. A* **2006**, *110*, 10163. hydrogen bonding to alkanes:(g) Olesen, S. G.; Hammerum, S. *J. Phys. Chem. A* **2009**, *113*, 7940 also refs 4 and 5a.

(7) The calculation of a hyperconjugative interaction $n(Y_{ax}) \rightarrow \sigma^*(C\text{-}H_{ax})$ is diagnostic for the presence of improper hydrogen bonding: (a) Reed, A. E.; Curtiss, L. A.; Weinhold, F. *Chem. Rev.* **1988**, *88*, 899. (b) Chocholoušová, J.; Špirko, V.; Hobza, P. *Phys. Chem. Chem. Phys.* **2004**, *6*, 37. (c) Nilsson, A.; Ogasawara, H.; Cavalleri, M.; Nordlund, D.; Nyberg, M.; Pettersson, L. G. M. *J. Chem. Phys.* **2005**, *122*, 154505. (d) Kryachko, E. S.; Zeegers-Huyskens, T. *J. Phys. Chem. A* **2002**, *106*, 6832.

(8) It is noted that changes of 0.1−1 ppm in the C−H proton chemical shift have been observed in a limited number of cases and are taken as evidence for the existence of C−H···O hydrogen bonds in solution. Intermolecular: (a) Xiang, S.; Yu, G.; Liang, Y.; Wu, L. *J. Mol. Struct.* **2006**, *789*, 43. (b) Wang, B.; Hinton, J. F.; Pulay, P. *J. Phys. Chem. A* **2003**, *107*, 4683. (c) Karger, N.; Amorim da Costa, A. M.; Ribeiro-Claro, P. J. A. *J. Phys. Chem. A* **1999**, *103*, 8672. (d) Mizuno, K.; Ochi, T.; Shindo, Y. *J. Chem. Phys.* **1998**, *109*, 9502. (e) Godfrey, P. D.; Grigsby, W. J.; Nichols, P. J.; Raston, C. L. *J. Am. Chem. Soc.* **1997**, *119*, 9283. Intramolecular: (f) Donati, A.; Ristori, S.; Bonechi, C.; Panza, L.; Nartini, G.; Rossi, C. *J. Am. Chem. Soc.* **2002**, *124*, 8778. (g) Barone, V.; Bolognese, A.; Correale, G.; Diurno, M. V.; Monterrey-Gomez, I.; Mazzoni, O. *J. Mol. Graph. Model.* **2001**, *19*, 318. (h) Nagawa, Y.;

Yamagaki, T.; Nakanishi, H.; Nakagawa, M.; Tezuka, T. *Tetrahedron Lett.* **1998**, *39*, 1393.

(9) See for example: Eliel, E. L.; Manoharan, M. *J. Org. Chem.* **1981**, *46*, 1959.

(10) (a) Engler, E. M.; Andose, J. D.; Schleyer, P. v. R. *J. Am. Chem. Soc.* **1973**, *95*, 8005. (b) Belanger-Giarepy, F.; Brisse, F.; Harvey, P. D.; Butler, I. S.; Gilson, D. F. R. *Acta Crystallogr.* **1987**, *C43*, 756.

(11) For the assignment and analysis of the ^{1}H NMR spectra of the 2-substituted adamantane derivatives see for example: (a) van Deursen, F. W.; Korver, P. K. *Tetrahedron Lett.* **1967**, 8145. (b) van Deursen, F. W.; Bakker, J. *Tetrahedron* **1971**, *27*, 4593. (c) Duddeck, H.; Hollowood, F.; Karim, A.; McKervey, M. A. *J. Chem. Soc. Perkin Trans 2* **1979**, 360. (d) Duddeck, H. *Top. Stereochem.* **1986**, *16*, 219. (e) Kolocouris, A. *Tetrahedron Lett.* **2007**, *48*, 2117.

(12) A preliminary study of this work has been reported: Zervos, N.; Kolocouris, A. *Tetrahedron Lett.* **2010**, *51*, 2453.

(13) Liu, S. B. *J. Chem. Phys.* **2007**, *126*, 244103.

(14) von Weizsäcker, C. F. *Z. Phys.* **1935**, *96*, 431.

(15) 6-31+G(d,p): Francl, M. M.; Pietro, W. J.; Hehre, W. J.; Binkley, J. S.; Gordon, M. S.; Defrees, D. J.; Pople, J. A. *J. Chem. Phys.* **1982**, *77*, 3654. MP2:Pople, J. A.; Binkley, J. S.; Seeger, R. *Int. J. Quantum Chem.* **1976**, *10* (S10), 1. B3LYP:(a) Becke, A. D. *J. Chem. Phys.* **1993**, *98*, 5648. (b) Lee, C. T.; Yang, W. T.; Parr, R. G. *Phys. Rev. B* **1988**, *37*, 785.

(16) Optimized geometries and NBO analyses were also performed at the B3LYP/6-31+G(d,p) level; the contact distances were longer and second order energies smaller (see the Supporting Information and also refs 2 and 12).

(17) Still the most popular source of van der Waals radii is an article by A. Bondii (Bondii, A. *J. Phys. Chem.* **1964**, *68*, 441) who gives the following values H, 1.20 Å; C, 1.70 Å; O, 1.52 Å; N, 1.55 Å; F, 1.47 Å; Cl, 1.75 Å; S, 1.80 Å; P, 1.80 Å; Si, 2.10 Å; using these values the sum of the van der Waals radii is, for example, 2.72 Å for H···O.

(18) Taylor, R.; Kennard, O. *J. Am. Chem. Soc.* **1982**, *104*, 5063.

(19) Calhorda, M. J. *Chem. Commun.* **2000**, 801 and references cited there in..

(20) (a) Novoa, J. J; Whangbo, M.-H.; Williams, J. M. *J. Chem. Phys.* **1991**, *94*, 4835. (b) Li, A. H.-T.; Chao, S. D. *J. Chem. Phys.* **2006**, *125*, 94312.

(21) Alkorta, I.; Elguero, J.; Grabowski, S. J. *J. Phys. Chem. A* **2008**, *112*, 2721.

(22) This is due to the borderline angle values for hydrogen bonding ($\theta_{C\text{-}H\cdots Y}$ = 95−98°).

(23) For calculations of C−H$_{ax}$···S contacts see for example ref 6d and Domagala, M.; Grabowski, S. J. *J. Phys. Chem. A* **2005**, *109*, 5683.

(24) What really determines the strength of the orbital interaction is the geometry of the overlapping orbitals $n(Y_{ax})$ and $\sigma^*(C-H_{ax})$ and not the relative orientation of the C−H and C−Y bond vectors. In this work, we concentrate in the second order perturbative energies that reflect the result/strength of the orbitals interactions. However, when the C−H and C−Y bond vectors are nearly parallel, the orbital interactions are weak, whereas the addition of an appropriate fragment X$_{ax}$ resulting in a X$_{ax}$−Y bond vector bisecting cyclohexane ring increases the energy stabilization as will be analyzed in the latter paragraphs of this work.

(25) Platts, J. A.; Howard, S. T.; Bracke, B. R. F. *J. Am. Chem. Soc.* **1996**, *118*, 2726.

(26) van den Berg, J.-A.; Seddon, K. R. *Cryst. Growth Des.* **2003**, *3*, 643.

(27) (a) Wennmohs, F.; Staemmler, V.; Schindler, M. *J. Chem. Phys.* **2003**, *119*, 3208. (b) Biswal, H. S.; Wategaonkar, S. *J. Phys. Chem. A* **2009**, *113*, 12763.

(28) The C−H···O contacts are the most common improper hydrogen bonded contacts encountered, especially the C−H···O═C contacts in proteins (see ref 3).

(29) (a) Liu, S. B.; Govind, N.; Pedersen, L. G. *J. Chem. Phys.* **2008**, *129*, 94104. (b) Liu, S. B.; Govind, N. *J. Phys Chem. A* **2008**, *112*, 6690. (c) Liu, S. B.; Hu, H.; Pedersen, L. G. *J. Phys Chem. A* **2010**, *114*, 5913. (d) Ess, D. H.; Liu, S.; De Proft, F. *J. Phys Chem. A* **2010**, *114*, 12952.

(30) Torrent-Sucarrat, M.; Liu, S.; De Proft, F. *J. Phys. Chem. A* **2009**, *113*, 3698.

(31) See for example: (a) Schleyer, P. v. R.; Maerker, C.; Dansfeld, A.; Jiao, H.; Hommes, N. J. R. v. E. *J. Am. Chem. Soc.* **1996**, *118*, 6317. (b) Abraham, R. J.; Griffiths, L.; Warne, M. A. *J. Chem. Soc., Perkin Trans, 2* **1997**, 31. (c) Sefzik, T. H.; Turco, D.; Iuliucci, R. J.; Facelli, J. C. *J. Phys. Chem. A* **2005**, *109*, 1180.

(32) See example: (a) Kolocouris, N.; Kolocouris, A.; Foscolos, G. B.; Fytas, G.; Neyts, J.; Padalko, E.; Balzarini, J.; Snoeck, R.; Andrei, G.; De Clercq, E. *J. Med. Chem.* **1996**, *39*, 3307. (b) Kolocouris, A.; Spearpoint, P.; Martin, S. R.; Hay, A. J.; López-Querol, M.; Sureda, F. X.; Padalko, E.; Neyts, J.; De Clercq, E. *Bioorg. Med. Chem. Lett.* **2008**, *18*, 6156. (c) Zoidis, G; Kolocouris, N.; Fytas, G.; Foscolos, G. B.; Kolocouris, A.; Fytas, G.; Karayannis, P.; Padalko, E.; Neyts, J.; De Clercq, E. *Antiviral Chem. Chemother.* **2003**, *14*, 155.

(33) Fry, J. L.; Engler, E. M.; Schleyer, P. v. R. *J. Am. Chem. Soc.* **1972**, *94*, 4628. Duddeck, H.; Rosenbaum, D. *J. Org. Chem.* **1991**, *56*, 1700.

(34) Oldenziel, O. H.; van Leusen, D.; van Leusen, A. M. *J. Org. Chem.* **1977**, *42*, 3114.

(35) Greidanus, J. W. *Can. J. Chem.* **1970**, *48*, 3593.

(36) Braga, D.; Chen, S.; Filson, H.; Maini, L.; Netherton, M. R.; Patrick, B. O.; Scheffer, J. R.; Scott, C.; Xia, W. J. *J. Am. Chem. Soc.* **2004**, *126*, 3511.

(37) Reed, A. E.; Curtiss, L. A.; Weinhold, F. *Chem. Rev.* **1988**, *88*, 899.

(38) Weinhold, F. In *Encyclopedia of Computational Chemistry*; Schleyer, P. v. R., Ed.; Wiley: New York, 1998; Vol. 3, p 1792.

(39) Reed., A. E.; Weinhold, F. *J. Chem. Phys.* **1985**, *83*, 1736.